Radiat Environ Biophys (2013) 52:411–417
DOI 10.1007/s00411-013-0474-9

SHORT COMMUNICATION

UV microspot irradiator at Columbia University

Alan W. Bigelow · Brian Ponnaiya · Kimara L. Targoff · David J. Brenner

Received: 8 February 2013 / Accepted: 13 May 2013 / Published online: 26 May 2013

Abstract The Radiological Research Accelerator Facility at Columbia University has recently added a UV microspot irradiator to a microbeam irradiation platform. This UV microspot irradiator applies multiphoton excitation at the focal point of an incident laser as the source for cell damage, and with this approach, a single cell within a 3D sample can be targeted and exposed to damaging UV. The UV microspot's ability to impart cellular damage within 3D is an advantage over all other microbeam techniques, which instead impart damage to numerous cells along microbeam tracks. This short communication is an overview, and a description of the UV microspot including the following applications and demonstrations of selective damage to live single cell targets: DNA damage foci formation, patterned irradiation, photoactivation, targeting of mitochondria, and targeting of individual cardiomyocytes in a live zebrafish embryo.

Keywords DNA damage · Microbeams · UV

Introduction

Continued development of innovative irradiation platforms has enhanced the array of irradiation modes available for radiation biology research at the Radiological Research Accelerator Facility (RARAF), Columbia University (Bigelow et al. 2011). While ion beams from the HVE 5.5 MeV Singletron particle accelerator at the facility also support secondary X-ray and neutron microbeam developments (Harken et al. 2011; Xu et al. 2011), a UV microspot irradiator is now combined with a charged-particle microbeam irradiator to enable experiments that require both photon and particle irradiations on the same platform. In contrast to cellular damage along the particle tracks from charged-particle microbeam irradiators, the UV microspot delivers damage through multiphoton excitation at localized cellular regions within a 3D sample. This integrated design allows the UV microspot to operate in two modes: (1) as a stand-alone UV microspot irradiator and (2) as a probe to work in concert with ion-beam irradiation experiments.

A. W. Bigelow (✉) · B. Ponnaiya · D. J. Brenner
Center for Radiological Research, Columbia University Medical Center, New York, NY, USA
e-mail: ab1260@columbia.edu

K. L. Targoff
Division of Pediatric Cardiology, Department of Pediatrics, College of Physicians and Surgeons, Columbia University, New York, NY 10032, USA

Materials and methods

The energy source for the UV microspot is a Chameleon Ultra II (Coherent, Inc., Santa Clara, CA, USA) tunable titanium–sapphire (Ti:S) laser which is part of a multiphoton microscope (Bigelow et al. 2008) and covers a wavelength range of 680–1,080 nm. While these long wavelengths allow for penetration depths of up to several hundred microns and are minimally damaging to a tissue sample, the two-photon and the three-photon processes effectively provide (340–540 nm) and (227–360 nm), respectively.

The volume of the UV microspot radiation is defined by the point spread function (PSF). Two-photon PSF measurements were obtained with 700 nm incident wavelength to image B200 Microgenics Corporation (Freemont, CA, USA) 0.2 μm diameter UV fluorescent beads through a water-immersion Plan Apo IR Nikon (Tokyo, Japan)

objective (60×, 1.27 NA). These PSF measurements were ellipsoids with <0.4 μm radial × 4.0 μm axial full-width half-maximum (FWHM) resolution. For comparison, three-photon PSF measurements using 1,000 nm excitation of the same UV beads through the same objective were ellipsoids with less than 0.4 μm radial × 3.0 μm axial FWHM resolution.

While single-photon excitation has a linear relationship with excitation laser power, the corresponding relationships for two-photon and three-photon excitation are quadratic and cubic, respectively. These two-photon and three-photon relationships were confirmed at RARAF through UV microspot excitation measurements of 10 μm diameter fluorescent UV beads. For the specific UV beads used in this test, the coefficient for the two-photon quadratic excitation trend was more than five orders of magnitude greater than the coefficient for the three-photon cubic excitation trend, indicating that a much greater photon flux is needed to induce three-photon excitation effects when compared to two-photon excitation effects.

An automated UV microspot irradiation protocol to sequentially identify and irradiate cellular targets is nearly identical to an established charged-particle microbeam protocol (Bigelow et al. 2011), except that the laser is applied during certain time intervals for desired exposures instead of a particle beam shuttered open for a desired number of particle counts. Automated and manual UV microspot irradiations of cellular systems can take place in air or in cell medium (using water-immersion objectives). UV microspot applications in concert with charged-particle microbeam irradiations require special thin-bottomed microbeam dishes that permit ion-beam transmission.

Results

A series of biology demonstrations is presented to showcase the capabilities of the UV microspot. The demonstrations include: (1) inducing single-strand DNA damage, (2) inducing DNA base damage, (3) patterned irradiation, (4) photoactivation of GFP within a single-cell nucleus, (5) targeting mitochondria, and (6) targeting embryonic zebrafish cardiomyocytes.

Inducing single-strand DNA damage

Human HT1080 fibrosarcoma cells that contain GFP-tagged XRCC1 single-strand DNA repair protein (developed by Dr. David Chen, UT Southwestern, Dallas, TX, USA) offer a model for imaging repair foci at radiation-induced DNA damage sites (Asaithamby and Chen 2011). HT1080 cell nuclei were targeted with the UV microspot irradiator to induce single-strand DNA breaks. The laser wavelength was tuned to 976 nm for the irradiation to potentially excite

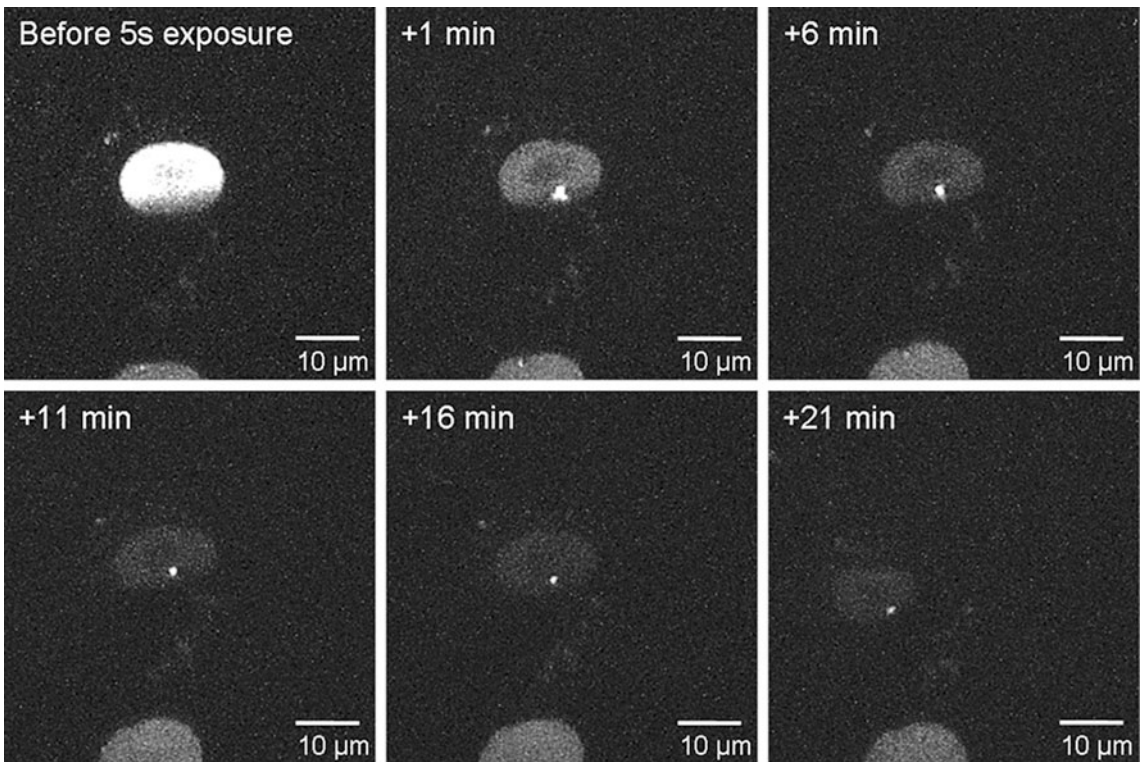

Fig. 1 Multiphoton microscope time-lapse images showing a single-cell nucleus before and after exposure to UV microspot

at: 1.27 eV (single photon), 2.54 eV (two photon), and 3.81 eV (three photon). The laser was focused through a 60× NA 1 water-immersion objective, irradiation time was 5 s, and laser power was set at 16 mW to deliver a UV microspot exposure energy of 80 mJ.

Multiphoton image stacks were taken before the irradiation and afterward in time-lapse mode (see Fig. 1) to capture the dynamics of XRCC1 repair following UV microspot exposure at a target position centered in the images shown in the time series. The time series depicts the rapid large-scale relocation of XRCC1 protein during the onset of the DNA repair focus of XRCC1 and the subsequent decay of the focus intensity. As there is variation in the stability of GFP expression per cell nucleus in this cell line (Asaithamby and Chen 2011), the nucleus with a large amount of XRCC1 protein (bright nucleus) in Fig. 1 was intentionally targeted for UV microspot irradiation in order to clearly demonstrate the rapid large-scale protein relocation phenomenon, which occurred for all irradiated nuclei.

Inspection of the individual images within a z-stack reveals structural detail in the repair focus. Figure 2 displays individual images, in 1 μm z-increments, from the "+1 min" z-stack image from Fig. 1. This series of optical sections transports the viewer through the cell nucleus and portrays structure in the focus, for instance, at the onset of the focus in the "$Z = 8$ μm" plane. In addition, there is a dark halo about the bright focus in each pane, which is possibly a manifestation of several multiphoton excitation modes within the cellular material.

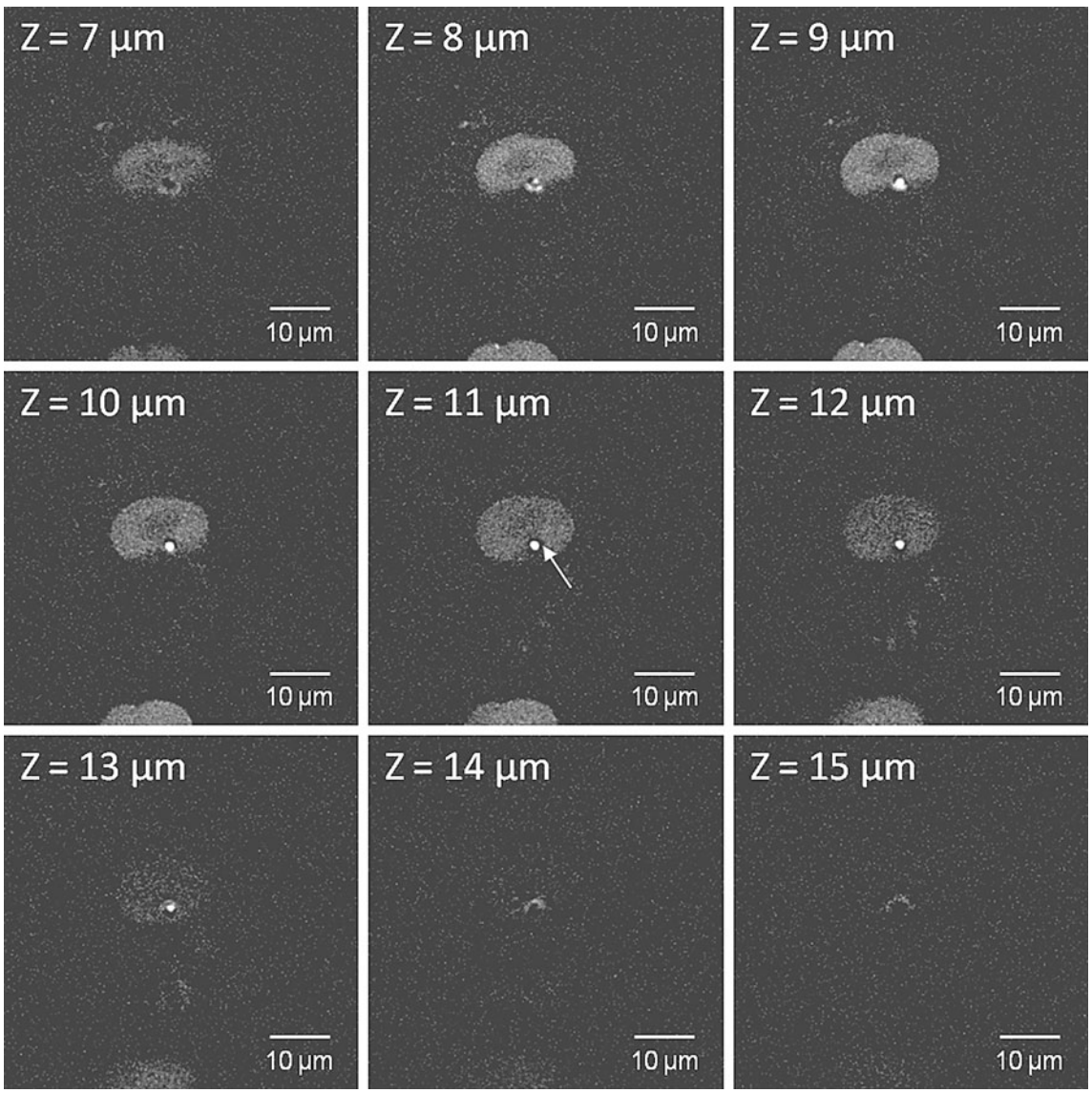

Fig. 2 Optical sections in steps of 1 μm of cell nucleus in Fig. 1 at +1 min following UV microspot irradiation. *Arrow* in the image ($Z = 11$ μm) indicates the dark halo region of diminished GFP fluorescence about the UV microspot-induced focus

Inducing DNA base damage

The UV microspot was used in a DNA base damage repair demonstration involving fluorescent protein attached to the base-repair protein 8-oxoguanine DNA glycosylase 1 (OGG1) in HT1080 fibrosarcoma cells. For UV microspot irradiation, the laser was tuned to 700 nm incident laser light to induce DNA damage in the cell nuclei. A 60× water-dipping lens transmitted 20 mW laser power during irradiation at 700 nm while the cell medium temperature was maintained at 37 °C. Cell nuclei were irradiated with varying numbers of 1-s duration line exposures across the frame of view. When exposure time was set for delivering 50 mJ energy across a cell nucleus, OGG1-foci formation was observed within an intact cell nucleus, as shown in the time-lapse multiphoton images in Fig. 3.

Patterned irradiation

The UV microspot irradiator can deliver user-defined exposure patterns to single cells either through mechanical stage motions or galvanometric mirror motions. Both pattern delivery options have been demonstrated using the HT1080 cell line described above. Through stage motions, the UV microspot irradiated the Columbia University crown logo into a live single-cell nucleus to produce a pattern of DNA repair foci (Bigelow et al. 2011). In a second demonstration of patterned irradiation, the laser exposure parameters (976 nm wavelength, 6.5 mW power, 20 s, 130 mJ) were maintained at a level to photobleach GFP while galvanometric mirror motions driven by perpendicular harmonic functions with a frequency ratio of 1:2 transmitted Lissajous figures into live HT1080 single-cell nuclei through a 60× NA 1.0 water-dipping objective. 3D z-stack images of the cell were acquired with multiphoton microscopy after the irradiation, and AutoQuant, an image debluring program, was used to optimize the image quality. Figure 4 shows the multiphoton microscopy images which are displayed as individual post-processed optical sections to transport the viewer through the cell containing a photobleached Lissajous figure imbedded in the nucleus. At the far right of Fig. 4, an overlay of the irradiated Lissajous pattern is indicated in the $Z = 4$ μm slice.

Photoactivation of GFP within a single-cell nucleus

In a photoactivation trial of GFP within a single cell, the UV microspot aimed at HeLa cells with photoactivable GFP in the nucleus that were provided by Michael Kruhlak at NIH/NCI. In this example, the cell in Fig. 5 was exposed

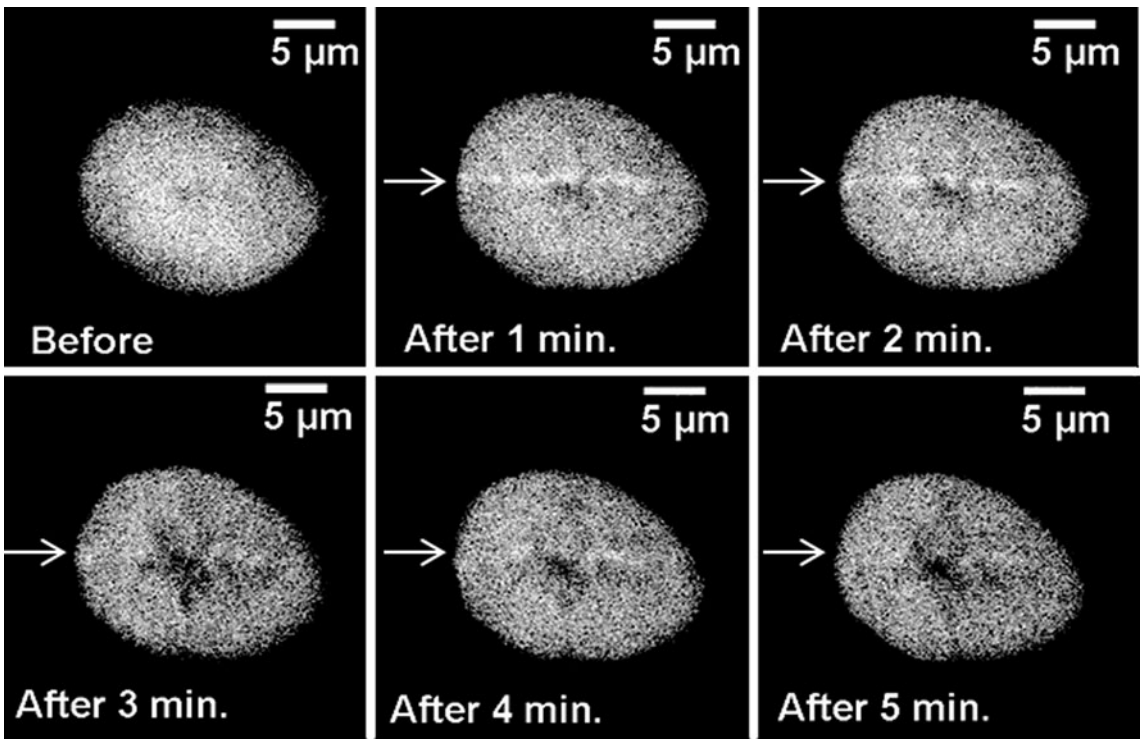

Fig. 3 Time-lapse multiphoton images of an HT1080 fibrosarcoma nucleus irradiated with the UV microspot. The irradiation pattern consisted of five line scans across the center of the cell nucleus. Energy delivered to the cell nucleus was approximately 50 mJ. The cell response is manifest by: (1) EGFP-tagged OGG1 foci formation along a *line* indicated by the *white arrows*, and (2) an intact nuclear membrane, suggesting cell viability

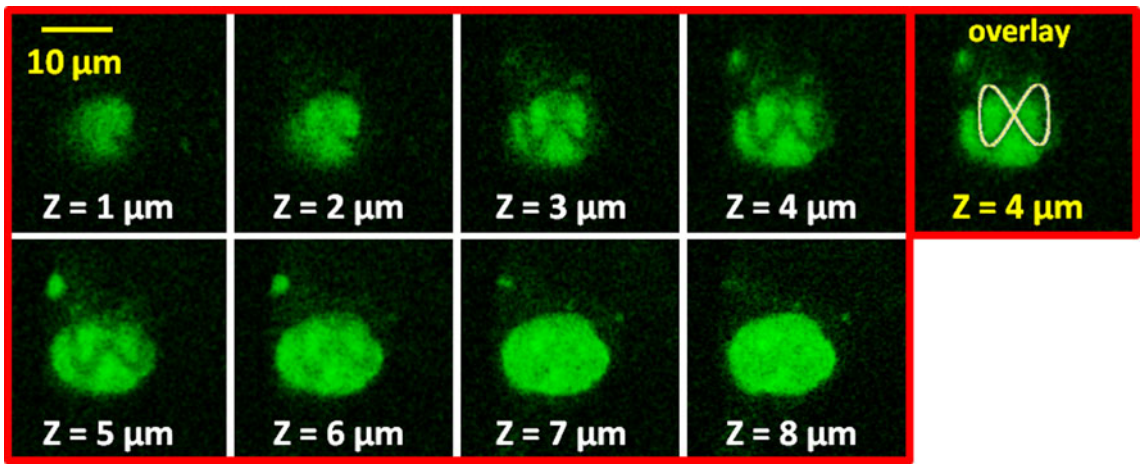

Fig. 4 Multiphoton images revealing photobleaching effects imbedded into a live single cell following UV microspot irradiation of a Lissajous pattern with 1:2 frequency ratio. An image at $z = 4$ µm with a Lissajous pattern overlay is also included

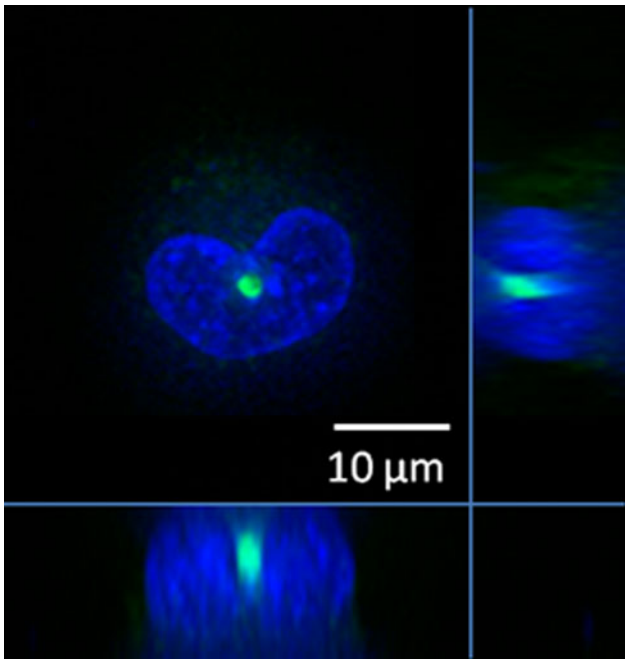

Fig. 5 Triple view of a live Hoechst-stained HeLa cell where the UV microspot photoactivated a volume within the cell that closely matched the PSF of the incident laser

to 37 mW power for 1 s, delivering 37 mJ exposure by the UV microspot tuned to 770 nm. Immediately after exposure, the cell was imaged with fluorescent z-stacks to visualize the photoactivated GFP spot within the Hoechst-stained cell nucleus. This image indicates a volume of GFP that closely matches the size of the laser PSF through the Nikon 60× NA 1 objective used for this trial; the full width at half-maximum values for that PSF were previously measured at 0.65 µm in the radial direction and 2 µm in the axial direction (Bigelow et al. 2008).

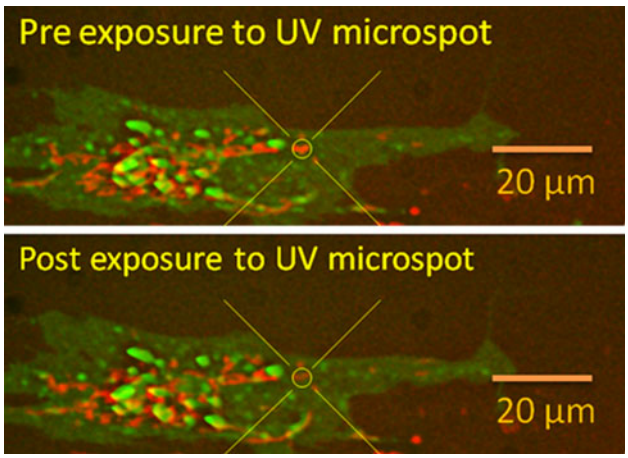

Fig. 6 Fluorescent images of a single AG1522 normal human skin fibroblast cell with targeted mitochondria region pre- and post-exposure to UV microspot irradiation

Targeting mitochondria

Imaging techniques for cellular organelles have facilitated precision microbeam irradiation of subcellular targets such as: mitochondria, lysosomes, actin, the Golgi apparatus, endoplasmic reticulum, and tubulin. The UV microspot irradiation of mitochondria demonstrates this imaging and targeting capacity for cellular organelles. In this demonstration, the AG1522 normal human skin fibroblast cell shown in Fig. 6 expressed mitochondria in RFP and lysosomes in GFP. A region of mitochondria was chosen for irradiation and positioned at the center of the crosshairs in the image to coincide with the UV microspot. Following UV microspot irradiation using a water-immersion Plan Apo IR Nikon objective, 60× NA 1.27 (1.5 s, 700 nm wavelength, 4.3 mW power, 6.5 mJ energy) photobleaching of the targeted mitochondria was confirmed.

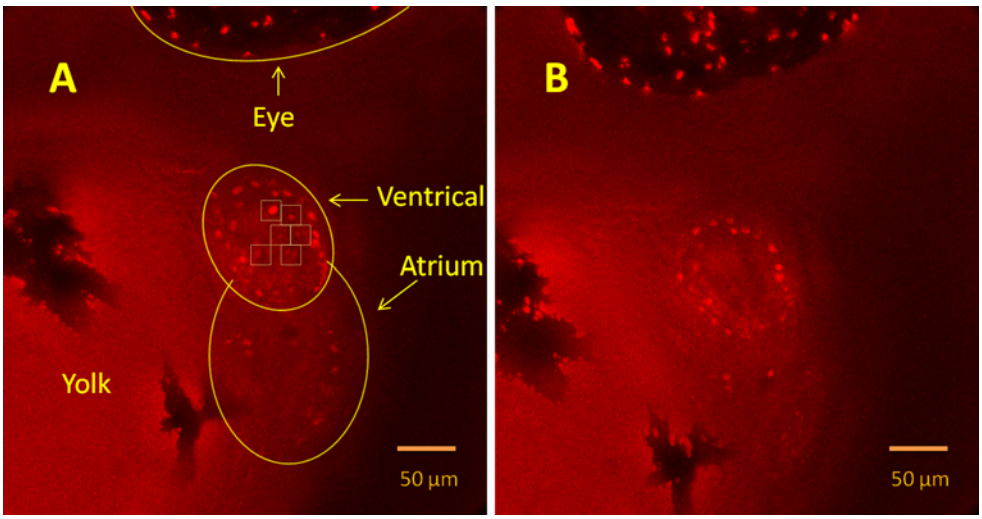

Fig. 7 Fluorescent z-stacks of a zebrafish embryonic heart before and after exposure to the UV microspot. All images were processed with AutoQuant software. See the text for descriptions to *panels* **a** and **b**

Targeting embryonic zebrafish cardiomyocytes

As samples for radiation biology experiments increase in complexity, studying radiation responses in tissue and in small organisms is becoming routine (Belyakov et al. 2005; Bertucci et al. 2009). Selective irradiation of specific cardiomyocytes in the zebrafish embryo has exemplified UV microspot irradiation of individual cells within a 3D structure. Individual cardiomyocyte nuclei in live zebrafish embryos carrying the transgene, *Tg(−5.1myl7:nDsRed2)*^{f2} (ZDB-ALT-060821-6) (Mably et al. 2003), are labeled through red fluorescence that can be imaged through conventional fluorescence microscopy. In preliminary studies, zebrafish embryonic heart cells were imaged using fluorescent z-stacks with a 20× NA 0.5 water-immersion objective before and after UV microspot irradiation. The exposure protocol involved imaging top surface ventricular cells and identifying six individual cell nuclei as targets. Each target was exposed to the UV microspot in a sequence of five coplanar 17.5 µm^2 scans (700 nm laser wavelength, 46 mJ total exposure energy, 18 mW exposure power, 2.56 s total exposure time).

In fluorescent z-stack images of a zebrafish embryo taken before and after UV microspot exposure (see Fig. 7), the cardiac chambers, a ventricle and an atrium, are clearly visible as well as the eyes and the yolk sack. The z-stacks in Fig. 7 comprise 120 µm of the sample and emphasize the targeted region of ventricular cardiomyocytes, before (Fig. 7a) and after (Fig. 7b) UV microspot exposure. Six yellow boxes overlayed on Fig. 7a each encompass a cell target and indicate the regions of UV microspot exposure. Figure 7b clearly shows that the targeted cells are no longer visible. This observation suggests damage to designated cell nuclei within a 3D organ and is the focus of ongoing studies on cell inactivation and cell ablation.

Conclusion

The Radiological Research Accelerator Facility at Columbia University has recently added a multiphoton excitation-based UV microspot irradiator to the available irradiation platforms for facility users. As the UV microspot irradiator produces cellular damage at the focal spot of an incident laser, a single cell within a 3D sample can be targeted and exposed to damaging UV while all neighboring cells are left unharmed. Applications for a UV microspot irradiator are vast and were presented with examples for DNA damage foci formation, patterned irradiation, photoactivation, targeting of mitochondria, and targeting of single cells on the heart of live zebrafish embryo.

Acknowledgments The authors thank: Asithambi Aroumougame from the David Chen group at UTSW for providing GFP-tagged XRCC1 HT1080 cells and EGFP-tagged OGG1 HT1080 cells; Iris Muller at GSI and Jonathan Chubb at the University of Dundee for providing a triple-tagged HT1080 cell line (RFP, YFP, and photoactivable GFP); and Michael Kruhlak at NIH/NCI for providing HeLa cells with photoactivable GFP. The authors also thank Columbia University employees Helen Turner for preparing and handling HT1080 cells, Vanessa George and Manuela Buonanno for preparing and handling the zebrafish embryo samples, and Gary Johnson for instrumentation development. This work was supported by the National Institute of Biomedical Imaging and Bioengineering under Grant: NIBIB 5P41 EB002033-16.

References

Asaithamby A, Chen DJ (2011) Mechanism of cluster DNA damage repair in response to high-atomic number and energy particles radiation. Mutat Res Fundam Mol Mech Mutagen 711(1–2):87–99

Belyakov OV, Mitchell SA, Parikh D, Randers-Pehrson G, Marino SA, Amundson SA, Geard CR, Brenner DJ (2005) Biological effects in unirradiated human tissue induced by radiation damage up to 1 mm away. Proc Natl Acad Sci USA 102(40):14203–14208

Bertucci A, Pocock RD, Randers-Pehrson G, Brenner DJ (2009) Microbeam irradiation of the *C. elegans* nematode. J Radiat Res 50(Suppl A):A49–A54

Bigelow AW, Geard CR, Randers-Pehrson G, Brenner DJ (2008) Microbeam-integrated multiphoton imaging system. Rev Sci Instrum 79(12):123707

Bigelow AW, Randers-Pehrson G, Garty G, Geard CR, Xu Y, Harken AD, Johnson GW, Brenner DJ (2011) Ion, X-ray, UV and neutron microbeam systems for cell irradiation. AIP Conf Proc 1336(1):351–355

Harken AD, Randers-Pehrson G, Johnson GW, Brenner DJ (2011) The Columbia University proton-induced soft X-ray microbeam. Nucl Instrum Method Phys Res Sect B 269(18):1992–1996

Mably JD, Burns CG, Chen J-N, Fishman MC, Mohideen M-APK (2003) Heart of glass regulates the concentric growth of the heart in zebrafish. Curr Biol 13(24):2138–2147

Xu Y, Randers-Pehrson G, Marino SA, Bigelow AW, Akselrod MS, Sykora JG, Brenner DJ (2011) An accelerator-based neutron microbeam system for studies of radiation effects. Radiat Prot Dosim 145(4):373–376